

Experiments With IDENTIKIT

Joshua E. Barnes¹ and George C. Privon²

¹*Institute For Astronomy, 2680 Woodlawn Drive, Honolulu, HI 96822, USA*

²*Department of Astronomy, University of Virginia, 530 McCormick Road, Charlottesville, VA 22904, USA*

Abstract. IDENTIKIT was originally developed as a fast approximate scheme for modeling the tidal morphology and kinematics of disk galaxy encounters and mergers. In this form, it was first used to implement an interactive modeling tool for galaxy collisions; tests with artificial data showed that the morphology *and* kinematics of merging galaxies strongly constrain their initial conditions. This tool is now being applied to real galaxies. More recently, IDENTIKIT has been used to develop a mapping from the present state of a tidal encounter back to the initial conditions; this offers a way to partly automate the search for dynamical models of galaxy encounters. Finally, IDENTIKIT's theoretical applications include a comprehensive way to evaluate the mass and extent of tidal features as functions of halo structure.

1. Introduction

The tidal theory of galaxy encounters explains the morphological and kinematic features of “peculiar” galaxies (Arp 1966) as consequences of gravitational interactions between previously normal disk galaxies (Toomre & Toomre 1972, hereafter TT72). While this theory has strong theoretical foundations, it gained considerable credibility from TT72's plausible simulations of four well-known interacting galaxies. In the decades since TT72, the number of systems with detailed dynamical models has gradually increased. There are several reasons, beyond testing the tidal theory, to create models of specific systems: such models (1) help interpret complex three-dimensional morphology, (2) provide access to the time domain, and (3) may be used to test sub-grid models of star formation, feedback, AGN fueling, etc. Thus, a dynamical merger model can provide a framework unifying disparate observations into a coherent picture.

Finding initial conditions which reproduce a specific pair of interacting galaxies is a time-consuming business. The parameter set is large, and parameters interact in complex ways. Hours may be required to run a single self-consistent calculation, and weeks of trial and error may be needed to obtain an acceptable match.

Sixteen parameters specify an encounter between two galaxies; these fall into three distinct groups as follows. (1) The initial orbit is specified by the pericentric separation p , mass ratio μ , and eccentricity e . (2) Disk orientations are specified by inclination angles i and azimuthal angles ϕ . (3) The mapping from a simulation to observables is specified by the time since pericenter t , three viewing angles θ_α , length and velocity scale factors \mathcal{L} and \mathcal{V} , position zero-point \mathbf{r}_0 and velocity zero-point \mathbf{v}_0 . Together, groups (1) and (2) specify the initial conditions.

The criteria used to decide if a model matches the observations are subtle. As a rule, it's not enough to reproduce the tidal morphology of an interacting pair of galaxies, since different encounter geometries may produce identical morphologies (e.g. Barnes 2011). Kinematic information on tidal bridges and tails provides much stronger constraints. Interferometric HI data, which traces both tidal morphology *and* kinematics, is often used to constrain merger models; H α may also be useful if tidal features contain emission-line regions. Molecular and/or stellar absorption lines can also provide constraints, but mapping extended structures in these lines is expensive. Models and observations are typically compared visually, for example by overplotting particles on various projections of a HI data cube (e.g. Hibbard & Mihos 1995). Since interstellar material converts between molecular, atomic, and ionized phases by processes outside the scope of purely dynamical models, visual inspection may be more reliable than quantitative measures derived by differencing model and observational data cubes. However, visual inspection is tedious and inherently subjective; robust quantitative methods would certainly be welcome.

Some progress has been made using genetic algorithms to automate the job of modeling interacting galaxies (e.g. Wahde 1998; Theis & Kohle 2001; Smith et al. 2010). Interesting results have been obtained, but most tests to date have searched only limited subsets of the relevant parameters and made little use of kinematic information.

2. IDENTIKIT 1

IDENTIKIT simulations combine test-particle and self-consistent techniques (Barnes & Hibbard 2009). Each galaxy is modeled by an initially spherical configuration of massive particles with cumulative mass profile $m(r)$, in which is embedded a spherical swarm of massless test particles on initially circular orbits. Two such models with mass ratio μ are launched towards each other on an orbit with eccentricity e and pericentric separation p . During the ensuing encounter, the massive components interact self-consistently, closely approximating the time-dependent potential and orbit decay of a fully self-consistent galactic collision. The test particles mimic the tidal response of embedded discs with all possible spin vectors; once such a simulation has been run, selecting the appropriate subset of test particles yields a good approximation to the tidal response of any particular disc.

Using this scheme, trial-and-error modeling of interacting galaxies becomes much less tedious. Barnes & Hibbard (2009) constructed an artificial data set of 36 parabolic ($e = 1$) encounters between equal-mass ($\mu = 1$) disk galaxies. The encounter geometries, pericentric separations, times since pericenter, viewing directions, and scale factors were chosen at random. With no knowledge of the actual parameter values, IDENTIKIT 1 was used to search for models reproducing the observable morphology and kinematics of these 36 systems. Some 30 cases were successfully reconstructed. In these cases, all unknown parameters were well-constrained; for example, encounter geometry and viewing direction were recovered with median errors of $< 15^\circ$.

2.1. Modeling real galaxies

Having passed “laboratory” tests, IDENTIKIT is ready to apply to real galaxies. This immediately raises several new issues. First is the limitations of the observational data. For most systems, HI is the only available tracer of large-scale morphology *and* kinematics. In many cases, the resolution and signal-to-noise of the data barely suffice to

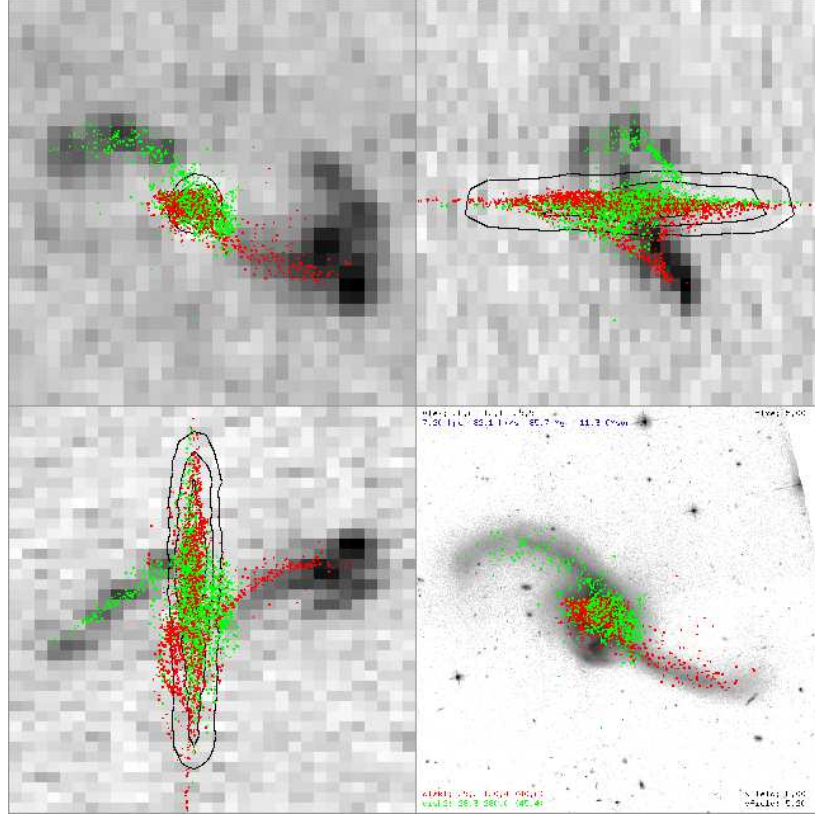


Figure 1. NGC 2623. Top-left and bottom-right panels show HI and optical images, respectively; North is up and West is right. Top-right and bottom-left panels show HI position-velocity diagrams; velocity increases to left and down, respectively. Grey-scale shows emission, while contours show HI absorption. Points show a preliminary IDENTIKIT 1 model (Privon et al., in preparation).

trace tidal structures. Second, the observational data may display features outside the scope of simple test-particle models. For example, HI data often includes absorption features, and it's not clear if or how such features can be matched by the simulations. Third, the mass models used in the IDENTIKIT simulations may not be good approximations to the actual mass distributions of the galaxies involved in an encounter. At this point, the simulations use generic disk galaxy models; tailoring these models to specific systems is an important challenge.

Fig. 1 presents a preliminary model of NGC 2623 (Privon et al., in preparation) which illustrates all three of these issues. First, while HI is definitely detected in the tails (Hibbard & Yun 1996), its emission is easier to map by taking the *maximum* voxel value along each line of sight through the data cube; summing the emission tends to produce noisy results. It's not entirely clear how to compare the present maps to the the projected particle distribution, which most naturally corresponds to summed emission. In addition, HI emission is not detected from the bright star-forming region to the south of the main body of NGC 2623; optical spectroscopy may help to determine kinematics

in this region. Second, the system exhibits HI absorption, presumably due to neutral hydrogen silhouetted against NGC 2623’s AGN (Evans et al. 2008). It’s interesting that the velocity width of this absorption feature is fairly well reproduced by the width of the particle distribution, but not entirely obvious that this is a success of the model since HI on the far side of the nucleus does not contribute to the absorption. Third, while NGC 2623 probably results from a merger of comparable galaxies, the hook-shaped tail to the West might be better reproduced if its parent galaxy’s disk was initially larger than its partner’s.

Further experience modeling a number of different systems is needed to explore these issues. It would also be interesting to combine HI with optical data, and to include other velocity tracers such as H α or CO. We are currently modeling Arp 240 (NGC 5257/8); other systems on our short-list include NGC 34 and NGC 3256. Eventually we hope to model a number of galaxies in the GOALS sample of luminous infrared galaxies (Armus et al. 2009).

3. IDENTIKIT 2

IDENTIKIT 2 (Barnes 2011) uses the self-consistent plus test-particle simulations described above to *solve* for the initial orientation of each disk. This offers a significant shortcut compared to the trial and error technique used with IDENTIKIT 1. The main assumption required is that the tidal features associated with each galaxy can be traced back to a single disk with a unique orientation.

To see how IDENTIKIT 2 works, consider a single region of phase space with finite extent in X , Y , and V_Z and infinite extent in the remaining dimensions. This region, hereafter called a “box”, is placed so as to sample the tidal material from a particular galaxy. At some time post-encounter, a single pass through the test-particle array for that galaxy selects *all* particles falling within the box. Each particle has been labeled with its initial spin axis relative to its parent galaxy, so the selected particles define a density distribution on the unit sphere of all possible spin directions. As a rule, this distribution is extended and does not define a unique orientation for the parent disk. However, *another* box sampling tidal material from the same disk will generate a different distribution, and the two distributions must overlap at the disk’s true orientation.

Given boxes tracing tidal features from both galaxies, IDENTIKIT 2 can solve for the inclinations and azimuths of both disks, directly determining four of the sixteen encounter and viewing parameters. The remaining twelve, however, must be specified beforehand, and if the specified values are wrong then the derived disk orientations will probably be wrong as well. But if *at least* three boxes – ideally more – are used to sample each disk, the effects of parameter mismatch tend to destroy the mutual overlap of the distributions. By quantifying how well the distributions overlap – for example, by forming the product of the densities they trace – a relative figure of merit for different solutions is obtained.

With a fairly robust method of measuring quality of fit, it’s possible to implement automatic searching over some subset of the twelve parameters besides disk orientation. Barnes (2011) described an implementation designed for systems composed of two disk galaxies which have not yet merged. In this version, just six parameters – the initial orbit (p , μ , e), time since pericenter t , velocity scale \mathcal{V} , and zero-point v_0 – must be specified ahead of time. In addition to a set of boxes tracing the tidal features of each galaxy, the algorithm requires coordinates on the plane of the sky for both galaxy

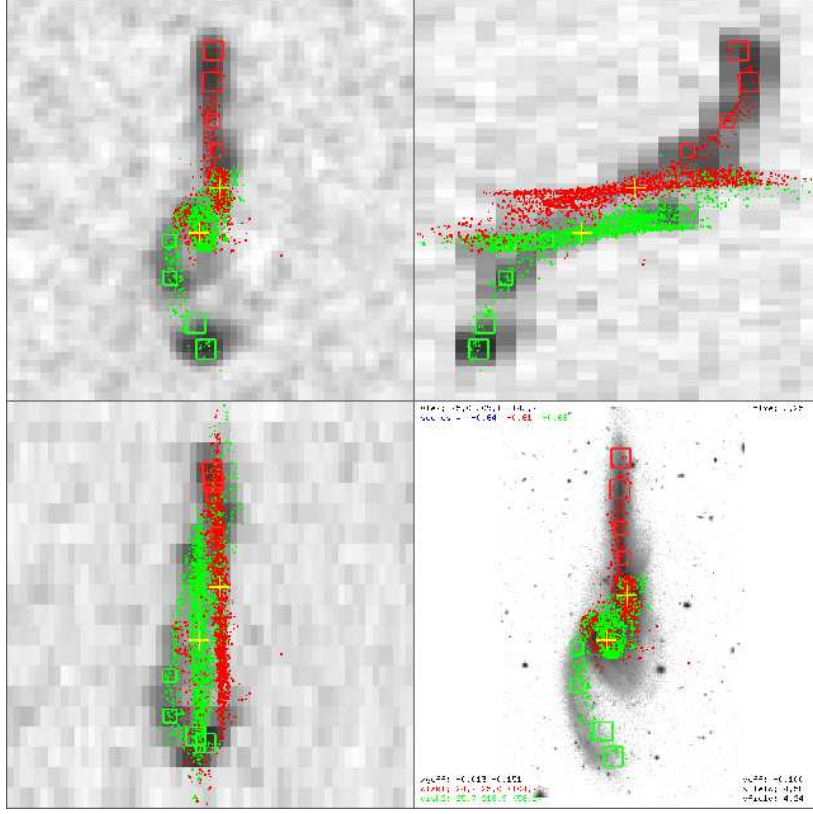


Figure 2. NGC 4676. Top-left and bottom-right panels show HI and optical images, respectively; North is up and West is right. Top-right and bottom-left panels show HI position-velocity diagrams; velocity increases to left and down, respectively. Boxes show constraints used to determine disk orientation. Points show IDENTIKIT 2 model.

nuclei. It performs a blind search over all possible viewing directions (θ_X, θ_Y); for each direction, the length scale \mathcal{L} , rotation about the line of sight θ_Z , and position zero-point \mathbf{r}_0 are determined by requiring the centers of the model galaxies to match the observed positions. Fits to both disks are scored independently as described above; the viewing direction which maximizes the product of both scores is selected. In tests with a small ensemble of simulated random mergers, the algorithm reconstructed encounter geometry and viewing direction with median errors of $< 8^\circ$.

Fig. 2 shows that the present algorithm already has interesting real-world applications. Here, four regions are allocated to each tail of “The Mice”, NGC 4676; these regions track the HI morphology and line-of-sight kinematics of the tails (Hibbard & van Gorkom 1996). In addition, the solution was constrained by requiring the simulated nuclei (crosses) to match the observed positions, and fall within the observed range of systemic velocities. Six parameters were specified a priori: the orbital eccentricity ($e = 1$), mass ratio ($\mu = 1$), pericentric separation (~ 4.5 disk scale lengths), time since pericenter (~ 1.25 disk rotation periods), velocity scale and velocity zero-point are close to the values adopted in earlier models (e.g. Barnes 2004). However, the remaining ten

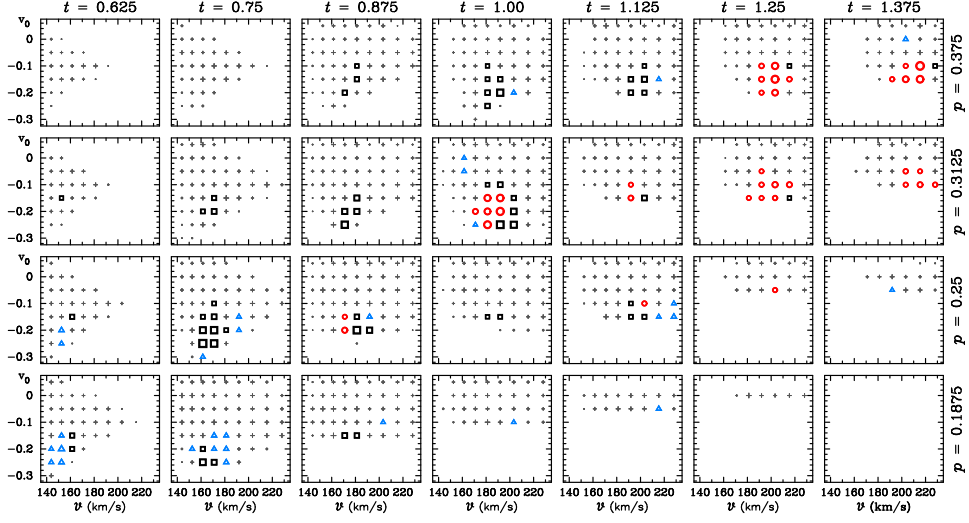


Figure 3. Fourteen-parameter search for models of NGC 4676. From one panel to the next, time since pericenter t increases left to right, and pericentric separation p increases bottom to top. Each panel shows a 9×8 grid of models in \mathcal{V} and v_0 . Symbol size indicates model score. The 122 highest-scoring solutions are visually classified as poor (triangles: $N = 30$), fair (squares: $N = 56$), and good (circles: $N = 36$); low-scoring solutions are shown as grey crosses.

parameters were all derived by the algorithm, which required about two minutes on a 2.16 GHz processor to examine 5120 viewing directions and produce the model shown here. This model is about as good as models of NGC 4676 derived by hand. Other “well-separated” systems which can be modeled in the same way include Arp 256, Arp 295, and Arp 298; HI data is available for all three.

3.1. Uniqueness and uncertainty

IDENTIKIT 2 is fast and robust enough to go beyond the ten-parameter search described above. For a system like NGC 4676, it’s reasonable to fix the mass ratio $\mu = 1$, adopt an $e = 1$ (parabolic) initial orbit, and perform a blind search in pericentric separation p , time since pericenter t , velocity scale \mathcal{V} , and velocity zero-point v_0 , as well as the angles θ_X and θ_Y defining direction of view. As the number of parameters to be determined increases, the algorithm yields solutions with comparable overall scores for many parameter combinations. In Fig. 3 solutions have been visually graded as poor, fair, or good representations of NGC 4676. It’s clear that numerical score is an imperfect indicator of quality, since the highest-scoring solutions (in the $t = 0.75$, $p = 0.25$ panel) are classified as fair, but many good solutions do get high scores, while poor solutions consistently get low scores.

The high-scoring solutions in Fig. 3 are not scattered at random; most fall along a diagonal from lower left to upper right across the panels, indicating a general correlation between time since pericenter t and pericentric separation p . Other parameters which correlate with t include the velocity zero-point v_0 , viewing angles (θ_X , θ_Y), and length and velocity scale factors \mathcal{L} and \mathcal{V} . These correlations indicate that acceptable solutions populate an “error ellipse” in parameter space. As a group, these solutions

are relatively homogeneous; they all appear to originate from a single connected region of parameter space. Moreover, the physical time since pericenter, $T = (\mathcal{L}/V)t$, is very well constrained; all of the good solutions and almost all of the fair ones yield T values between 150 and 200 Myr.

Although it may seem better to obtain a unique model, the ensemble of solutions for NGC 4676 shown in Fig. 3 is probably a good representation of the actual uncertainties inherent in modeling this system with available HI data. There’s no telling if most interacting galaxies will likewise yield fairly well-constrained solutions; NGC 4676 is a relatively simple system, and others may be harder to constrain.

This 14-parameter search shows that comprehensive surveys of the encounter parameter space are possible. While the *internal* structures of the victim galaxies remain to be parametrized (§ 4), the ability to search such large spaces is encouraging.

4. Mass models

The results presented above use a generic galaxy model with a bulge+disk:halo mass ratio $(m_b + m_d) : m_h = 1 : 4$. While this model is adequate for some purposes, the halo comprises just 80% of the total, which is less than expected in CDM cosmologies. Moreover, any effort at data-driven modeling of real mergers must address variations in initial galaxy structure. How sensitive are model results to inevitable discrepancies between the adopted and actual structure of the progenitor galaxies? Can tidal encounter models accurately probe the overall depth and structure of halo potential wells?

Existing work on the effects of halo structure on tidal features (Dubinski et al. 1996, 1999; Springel & White 1999) has largely focused on direct, co-planar encounters which maximize tidal features; a systematic study varying encounter geometry as well as galaxy structure is bedeviled by a large number of parameters. However, IDENTIKIT offers an efficient way to treat encounter geometry, since a single simulation simultaneously models all possible disk orientations. Fig. 4 presents an example, based on a galaxy model with mass ratio $(m_b + m_d) : m_h = 1 : 9$. The plot shows test particles which have attained a maximum distance from their parent galaxy of at least three times their initial orbital radius; these particles populate tidal features. Particles are classified as belonging to bridge or tail structures based on their position relative to the two galaxies at (1) first passage and (2) instant of maximum distance; a very few particles don’t belong to either. No selection for initial disk orientation is done, so the result is a “synoptic” view of *all* tidal structures resulting from this encounter.

The histogram on the right of Fig. 4 shows how the mass fractions μ_{tid} in bridges and tails depend on disk inclination i . At small inclinations ($i < 30^\circ$), the bridge is relatively massive, comprising $\sim 8\%$ of the disk material. However, bridge mass drops rapidly with increasing i . The tail is less massive, amounting to $\sim 2.5\%$ of the disk material for small i , but drops off less rapidly with increasing i . In effect, bridge-to-tail mass ratio is a decreasing function of inclination; this trend would be very difficult to quantify using conventional simulations.

References

- Armus, L., Mazzarella, J. M., Evans, A. S., Surace, J. A., Sanders, D. B., Iwasawa, K., Frayer, D. T., Howell, J. H., Chan, B., Petric, A., Vavilkin, T., Kim, D. C., Haan, S., Inami, H., Murphy, E. J., Appleton, P. N., Barnes, J. E., Bothun, G., Bridge, C. R., Charmandaris,

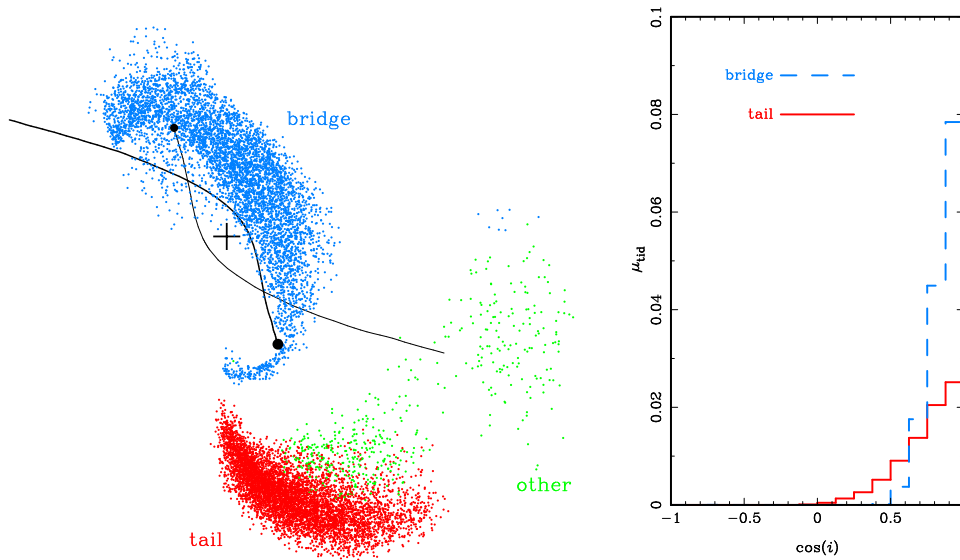


Figure 4. Left: result of a moderately close passage between two equal-mass galaxies, seen shortly after apocenter. Solid lines are galaxy trajectories; the cross marks the system's center of mass. Points show tidal structures originating from the galaxy marked by the larger filled circle, integrated over all possible disk orientations; bridge and tail particles populate distinct regions as shown. Right: histogram showing bridge and tail mass fractions as functions of disk inclination i .

V., Jensen, J. B., Kewley, L. J., Lord, S., Madore, B. F., Marshall, J. A., Melbourne, J. E., Rich, J., Satyapal, S., Schulz, B., Spoon, H. W. W., Sturm, E., U, V., Veilleux, S., & Xu, K. 2009, *PASP*, 121, 559

Arp, H. 1966, *ApJS*, 14, 1

Barnes, J. E. 2004, *MNRAS*, 350, 798

— 2011, *MNRAS*, 413, 2860

Barnes, J. E., & Hibbard, J. E. 2009, *AJ*, 137, 3071

Dubinski, J., Mihos, J. C., & Hernquist, L. 1996, *ApJ*, 462, 576

— 1999, *ApJ*, 526, 607

Evans, A. S., Vavilkin, T., Pizagno, J., Modica, F., Mazzarella, J. M., Iwasawa, K., Howell, J. H., Surace, J. A., Armus, L., Petric, A. O., Spoon, H. W. W., Barnes, J. E., Suer, T. A., Sanders, D. B., Chan, B., & Lord, S. 2008, *ApJ*, 675, L69

Hibbard, J. E., & Mihos, J. C. 1995, *AJ*, 110, 140

Hibbard, J. E., & van Gorkom, J. H. 1996, *AJ*, 111, 655

Hibbard, J. E., & Yun, M. S. 1996, in *Cold Gas at High Redshift*, edited by M. N. Bremer & N. Malcolm, vol. 206 of *Astrophysics and Space Science Library*, 47

Smith, B. J., Carver, D. C., Pfeiffer, P., Perkins, S., Barkanic, J., Fritts, S., Southerland, D., Manchikalapudi, D., Baker, M., Luckey, J., Franklin, C., Moffett, A., & Struck, C. 2010, in *Galaxy Wars: Stellar Populations and Star Formation in Interacting Galaxies*, edited by B. Smith, J. Higdon, S. Higdon, & N. Bastian, vol. 423 of *Astronomical Society of the Pacific Conference Series*, 227

Springel, V., & White, S. D. M. 1999, *MNRAS*, 307, 162

Theis, C., & Kohle, S. 2001, *A&A*, 370, 365

Toomre, A., & Toomre, J. 1972, *ApJ*, 178, 623

Wahde, M. 1998, *A&AS*, 132, 417